Shell-Model Description of Weakly Bound Nuclei

Nicolas Michel*, Witold Nazarewicz† and Marek Płoszajczak*

*GANIL, CEA/DSM-CNRS/IN2P3, BP 5027, F-14076 Caen Cedex 05, France
†Department of Physics and Astronomy, The University of Tennessee, Knoxville, Tennessee 37996
Physics Division, Oak Ridge National Laboratory, P.O. Box 2008, Oak Ridge, Tennessee 37831
Institute of Theoretical Physics, Warsaw University, ul. Hoża 69, PL-00681, Warsaw, Poland

Abstract. This work presents the first continuum shell-model study of weakly bound neutron-rich nuclei with *several* valence nucleons. For the single-particle basis, we take the complex-energy Berggren ensemble representing the bound single-particle states, narrow resonances (Gamow states), and the non-resonant continuum. In our calculations, we consider the shell-model Hamiltonian consisting of a one-body finite Woods-Saxon potential and a residual two-body interaction. The proposed Gamow shell model, which is a straightforward extension of the traditional shell model based on a discrete basis, is shown to be an excellent tool for the microscopic description of weakly bound systems.

INTRODUCTION

It is a great pleasure to dedicate this paper to Rick Casten on the occasion of this conference in his honor. The subject of our work, i.e., the shell-model treatment of exotic nuclei, is of particular relevance to Rick's anniversary. Firstly, the nuclear shell model has been a guiding principle behind most of his scientific work [1]. Secondly, the physics of exotic nuclei far from the beta stability line has been one of Rick's main scientific interests and activities [2].

In many respects, weakly bound nuclei are much more difficult to treat theoretically than well-bound systems [3]. The major theoretical difficulty and challenge is the treatment of the particle continuum. For weakly bound nuclei, the Fermi energy lies very close to zero, and the decay channels must be taken into account explicitly. As a result, many cherished approaches of nuclear theory such as the conventional shell model and the pairing theory must be modified. But there is also a splendid opportunity: the explicit coupling between bound states and continuum, and the presence of low-lying scattering states invite strong interplay and cross-fertilization between nuclear structure and reaction theory. Many methods developed by reaction theory can now be applied to structure aspects of loosely bound systems. And, of course, nuclear structure effects can clearly manifest themselves in reactions involving exotic nuclei.

The treatment of continuum states is an old problem which, in the context of excited states near or above the decay threshold, has been a playground of the continuum shell model (CSM) [4]. In the CSM, including the recently developed Shell Model Embedded in the Continuum (SMEC) [5], the scattering states and bound states are treated on an equal footing. So far, most applications of the CSM, including SMEC, have been used to describe limiting situations in which there is coupling to *one-nucleon decay*

channels only. However, by allowing only one particle to be present in the continuum, it is impossible to apply the CSM to 'Borromean systems' for which A- and $(A$-2)-nucleon systems are particle-stable but the intermediate $(A$-1)-system is not. Various approaches, including the hyperspherical harmonic method or the coupled-channel approach, have been developed to study structure and reaction aspects of three-body weakly bound nuclei [6]. However, most of these models utilize the particle-core coupling which does not allow for the exact treatment of core excitations and the antisymmetrization between the core nucleons and the valence particles.

The reason for limiting oneself to only one particle in the continuum in the CSM has been two-fold. First, the number of scattering states needed to properly describe the underlying dynamics can easily go beyond the limit of what present computers can handle. Second, treating the continuum-continuum coupling, which is always present when two or more particles are scattered to unbound levels, is difficult. There have been only a few attempts to treat the multi-particle case and, unfortunately, the proposed numerical schemes, due to their complexity, have never been adopted in microscopic calculations involving multiconfiguration mixing. Consequently, an entirely different approach is called for. Recently, we formulated and tested the multiconfigurational shell model in the complete Berggren basis [7], the so-called Gamow Shell Model (GSM). (For application to two-particle resonant states, see also Ref. [8].) In this paper, GSM is applied to systems containing several valence neutrons.

BERGGREN BASIS AND COMPLETENESS RELATIONS

The Gamow states (sometimes called Siegert or resonant states) [9] are generalized eigenstates of the time-independent Schrödinger equation with complex energy eigenvalues $E = E_0 - i\Gamma/2$, where Γ stands for the decay width (which is zero for bound states). These states correspond to the poles of the S-matrix in the complex energy plane lying on or below the positive real axis; they are regular at the origin and satisfy purely outgoing asymptotics. Figure 1 shows the distribution of Gamow states in the complex momentum plane.

In the following, we consider the Gamow states of a one-body spherical finite potential. The single-particle (s.p.) basis of Gamow states must be completed by means of a set of non-resonant continuum states. This completeness relation [10, 11], reads:

$$\sum_n |\phi_{nj}\rangle\langle\tilde{\phi}_{nj}| + \frac{1}{\pi}\int_{L_+} |\phi_j(k)\rangle\langle\phi_j(k^*)|\,dk = 1, \tag{1}$$

where ϕ_{nj} are the Gamow states carrying the s.p. angular momentum j, n stands for all the remaining quantum numbers labeling Gamow states, $\phi_j(k)$ are the modified scattering Gamow states, and the contour L_+ in the complex k-plane has to be chosen in such a way that all the poles in the discrete sum in Eq. (1) are contained in the domain between L_+ and the real energy axis (cf. Fig. 1). If $u_{nj}(r)$ stands for the radial part of ϕ_{nj}, then $\tilde{u}_{nj}(r) = u_{nj}(r)^*$ and $\tilde{\phi}_{nj}$=$\phi_{nj}(u \to \tilde{u})$. If the contour L_+ is chosen reasonably close to the real energy axis, the first term in (1) represents the contribution from bound states and narrow resonances, while the integral part accounts for the non-resonant

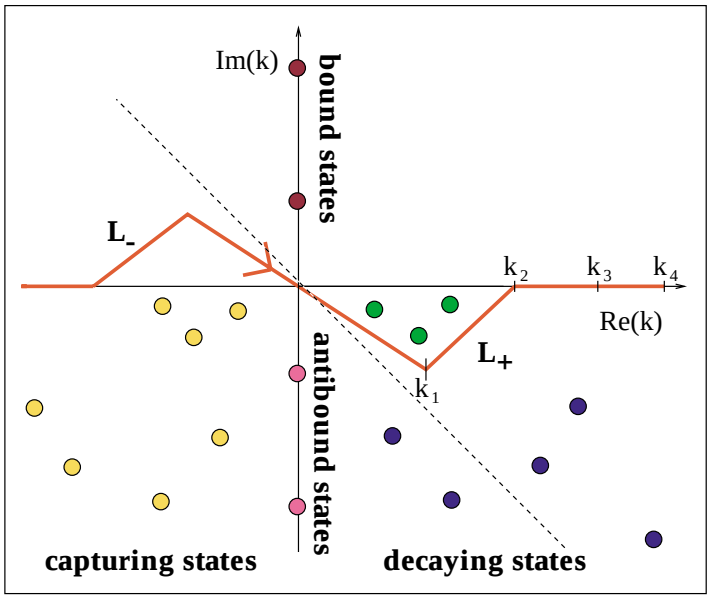

FIGURE 1. Schematic representation of the Gamow basis in the complex momentum plane. The Gamow states (i.e., poles of the S-matrix) are indicated by dots: bound states ($k = i\gamma$), antibound states ($k = -i\gamma$), decaying resonances ($k = \kappa - i\gamma$), and capturing resonances ($k = -\kappa - i\gamma$). The contour L represents the non-resonant continuum (see Eq. 1).

continuum. A number of completeness relations similar to (1) were studied by Lind [11]. In particular, if L_+ coincides with the real axis, one obtains the well-known Newton completeness relation involving bound and scattering states:

$$\sum_{n=\text{bound}} |\phi_{nj}\rangle\langle\tilde{\phi}_{nj}| + \frac{1}{\pi}\int_R |\phi_j(k)\rangle\langle\phi_j(k^*)|\,dk = 1. \tag{2}$$

There have been several applications of resonant states to problems involving continuum [12], but in most cases the so-called *pole expansion*, neglecting the contour integral in Eq. (1), was used. The importance of the contour contribution was investigated in Refs. [13, 14] in the context of the continuum RPA with separable particle-hole interactions where it was concluded that the non-resonant part must be accounted for if one aims at a quantitative description. This can be achieved by discretizing the integral in Eq. (1) [15]. In this work, we use the quadrature based on the four-point interpolation. The number of discretization points in the non-resonant scattering continuum is denoted by N_{cont} in the following.

In our study, Gamow states are determined using the generalized shooting method for bound states which requires an exterior complex scaling [12]. The antisymmetric two-particle wave functions $|\phi^{(1)}_{i_1}\,\phi^{(2)}_{i_2}\rangle_J$ are obtained in the usual way by coupling the s.p. wave functions of the considered bound, resonance, and scattering Gamow states. The radial integrals entering the Hamiltonian matrix elements were regularized separately by an appropriate choice of the angle of the exterior complex scaling. The resulting

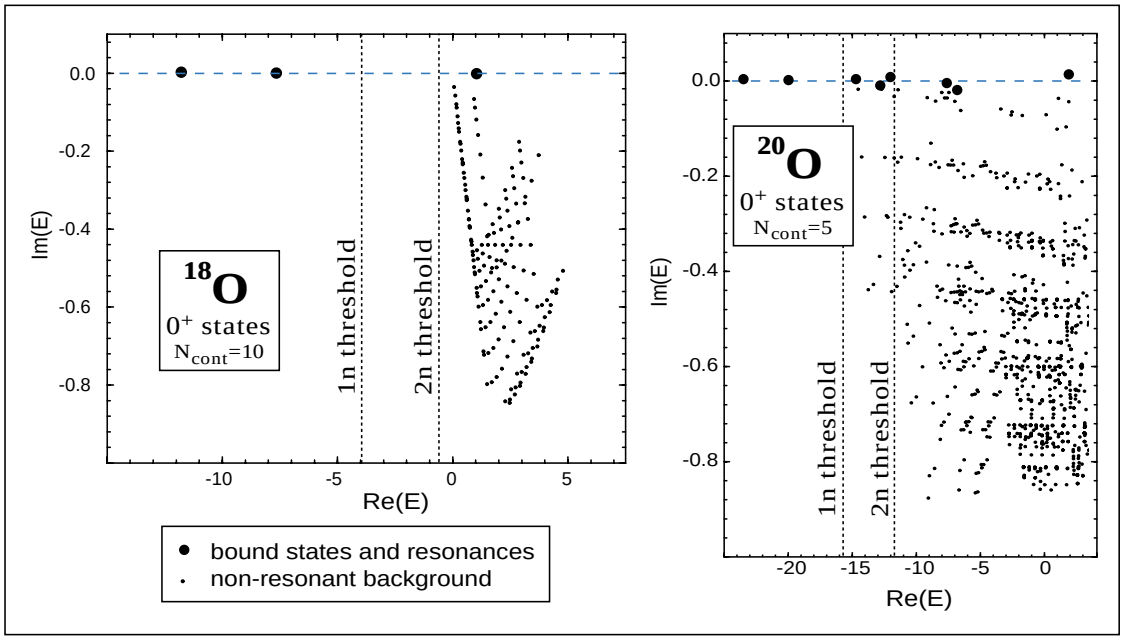

FIGURE 2. Distribution of GSM states in the complex energy plane calculated for ^{18}O (left; (two-particle case) and ^{20}O (right; four particle case). The bound and resonant states lie close to the real energy axis; they are marked by large dots. The remaining states represent the non-resonant continuum. One- and two-neutron thresholds are indicated.

(complex symmetrix) Hamiltonian matrix can be diagonalized using standard methods [7].

SELECTION OF RESONANT STATES

The crucial problem pertaining to the interpretation of the CSM results is the selection of states associated with resonant excitations of the system. Bound states can be clearly identified, because the imaginary part of their energy must be zero. No equally simple criterion exists for resonance states. Fortunately, the coupling between scattering states and resonant states is usually weak; hence, one can determine the resonances using the following two-step procedure. In the first step, the shell-model Hamiltonian is diagonalized in both (i) the full space including the contour, and (ii) the subspace of Gamow states (pole expansion). In the second step, one identifies the eigenstates of (i) which have the largest overlap with those of the second diagonalization. As a representative example, Fig. 2 shows the distribution of shell-model energies in the complex energy plane calculated for ^{18}O and ^{20}O. In both cases the bound states and resonances lie at, or very close to, the real energy axis. The remaining states represent the non-resonant continuum; their distribution varies with $N_{\rm cont}$. On the other hand, bound and resonant states are stable with respect to $N_{\rm cont}$. All states below the one-neutron threshold (marked as 1n) are bound. The states above the two-neutron (2n) threshold are unstable to one- and two-neutron emission. As seen in Fig. 2, for ^{18}O, the eigenstates forming the non-

resonant background align along regular trajectories in the complex energy plane [8] that reflect the choice of the contour L_+ in the momentum space. In the four-particle case, ^{20}O, this regularity is practically lost.

EXAMPLES OF CALCULATIONS

In the following exploratory GSM calculations, we shall consider two cases: (i) $^{18-22}$O with the inert ^{16}O core and active neutrons in the *sd* shell, and (ii) $^{6-9}$He with the inert ^{4}He core and active neutrons in the *p* shell. Our aim is not to give the precise description of these nuclei (for this, one would need a realistic Hamiltonian and a larger configuration space), but rather to illustrate the method, its basic ingredients, and underlying features. The details of these calculations will be published elsewhere [16].

The “Oxygen" case

The s.p. basis was generated by a Woods-Saxon (WS) potential with the radius R_0=3.05 fm, the surface diffuseness d=0.65 fm, the potential depth U_0=–55.8 MeV, and the strength of the spin-orbit term U_{so}=6.06 MeV. With this choice of parameters, the single particle $0d_{5/2}$ and $1s_{1/2}$ states are bound with s.p. energies -4.14 MeV and -3.27 MeV, respectively, and $0d_{3/2}$ is a resonance with the s.p. energy 0.9–i0.048 MeV. Energies of these s.p. states are close to the s.p. states of ^{17}O. The completeness relation requires taking the $s_{1/2}$, $d_{5/2}$, and $d_{3/2}$ non-resonant continuums. For the $1s_{1/2}$ and $0d_{5/2}$ bound states, their non-resonant continuums can be chosen along the real momentum axis. Since, to the first order, the inclusion of these continuums should only result in the renormalization of the effective interaction, they are ignored for the purpose of the present exercise whose main focus is the neutron emission. On the contrary, $0d_{3/2}$ is a resonance state, so the associated contour has to be complex to produce the correct energy width. The number of discretization points was $N_{\rm cont}$=5. For the residual interaction, we assumed the δ-force with the strength V_0=-350 MeV fm^3.

Figure 3 displays binding energies of $^{18-22}$O calculated in GSM. In spite of very simple interaction and rather limited configuration space, the agreement with experimental data is good. Also quite reasonable is the predicted spectrum of ^{18}O (Fig. 3, inset). In particular, the states which are predicted to appear above the 1n threshold acquire a positive width [7].

The “Helium" case

A description of the neutron-rich helium isotopes, including Borromean nuclei ^{6,8}He, is a challenge for the GSM. ^{4}He is a well-bound system with the one-neutron emission threshold at 20.58 MeV. On the contrary, the nucleus ^{5}He, with one neutron in the *p* shell, is unstable with respect to the neutron emission. Indeed, the $J^\pi = 3/2^-_1$ ground

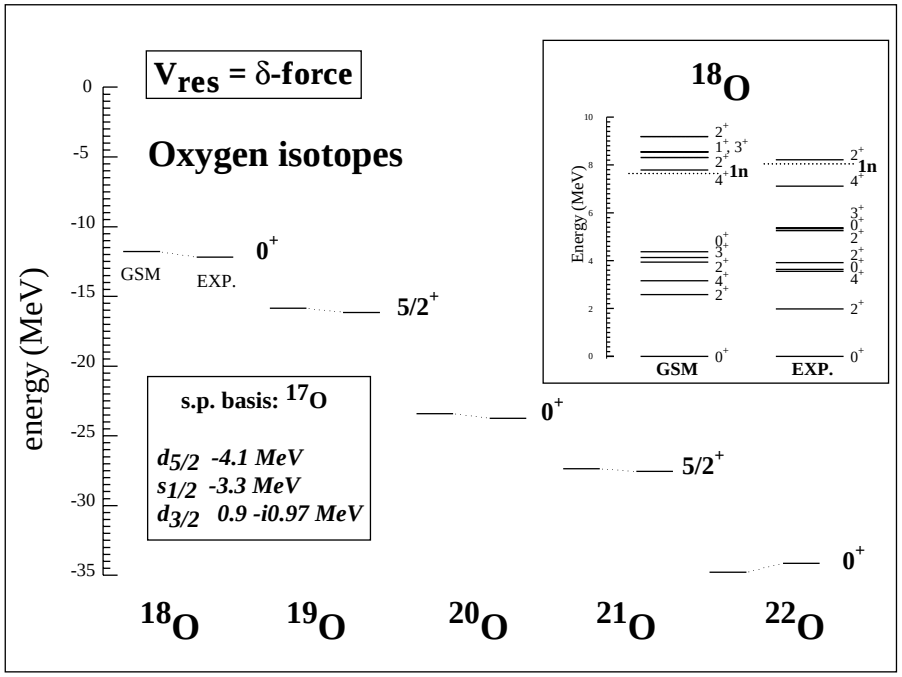

FIGURE 3. Experimental (EXP) and predicted(GSM) binding energies of $^{18-22}$O. The inset shows the calculated two-neutron spectrum of ^{18}O compared to experimental data.

state of ^{5}He lies 890 keV above the neutron emission threshold and its neutron width is large, Γ=600 keV. The first excited state, $1/2^-_1$, is a very broad resonance (Γ=4 MeV) that lies 4.89 MeV above the threshold. ^{6}He, on the contrary, is bound with the two-neutron emission threshold at 0.98 MeV and one-neutron emission threshold at 1.87 MeV. The first excited state 2^+_1 at 1.8 MeV in ^{6}He is neutron unstable with a width Γ=113 keV. In our GSM calculations, the states in ^{5}He are viewed as one-neutron resonances outside of the ^{4}He core. A good fit to $3/2^-_1$ and $1/2^-_1$ states in ^{5}He is obtained by taking the WS potential with R_0 = 2 fm, d=0.65 fm, U_0 = -47 MeV, and U_{so} = 7.5 MeV. With this potential, one finds the single-neutron resonances $p_{3/2}$ and $p_{1/2}$ at E=0.745–i0.32 MeV and E=2.13–i2.94 MeV, respectively. The number of discretization points was $N_{\rm cont}$=5 for both partial waves. With this choice of $N_{\rm cont}$=5 the accuracy of calculations (i.e., the size of the false width) was of the order of 100 keV. For the residual interaction, we assumed the surface-delta interaction (SDI) with the strength V_0=-1670 MeV fm^3 and radius R=2 fm.

Our calculations reproduce the most important feature of ^{6}He and ^{8}He: *the ground state is particle-bound, despite the fact that all the basis states lie in the continuum.* In spite of a very crude Hamiltonian, rather limited configuration space, etc., the calculated ground state energies reproduce surprisingly well the experimental data. The neutron separation energy anomaly (i.e., the *increase* of the neutron separation energy when going from ^{6}He to ^{8}He) is reproduced. Also, the energies of excited 2^+_1 states are in fair agreement with the data. As discussed in Refs. [7, 16], the contribution from the non-resonant continuum to the ground state wave functions of Borromean systems ^{6}He

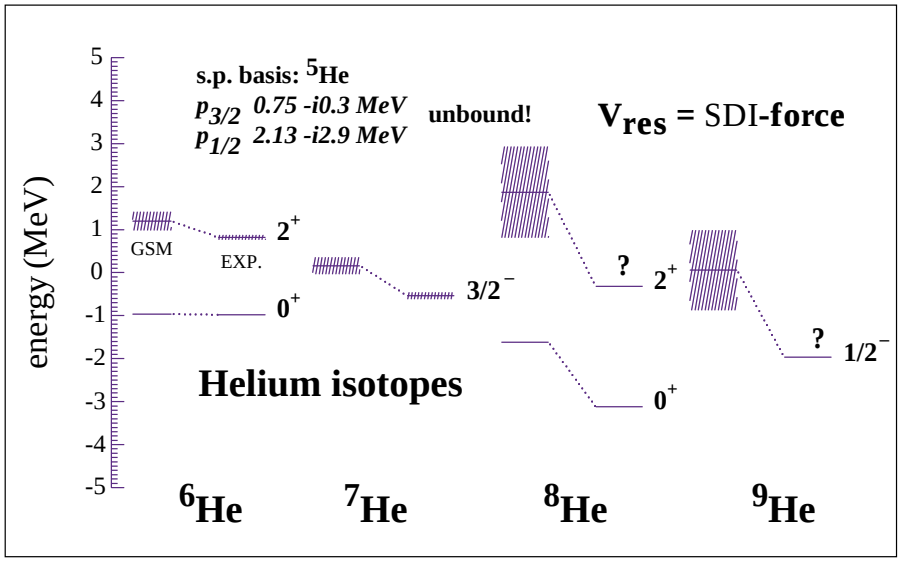

FIGURE 4. Experimental (EXP) and predicted(GSM) binding energies of $^{6-9}$He as well as energies of J^{π}=2^{+} states in ^{6,8}He. The resonance widths are indicated by shading.

and ^{8}He is large. As seen in Table 1, the contributions from one and two particles in the non-resonant continuum, $L_{+}^{(1)}$ and $L_{+}^{(2)}$, dominate the structure of the ground-state wave function of ^{8}He.

TABLE 1. Squared complex amplitudes of different configurations in 0_1^+ and 2_1^+ states of ^{8}He. The sum of squared amplitudes of all Slater determinants including n particles in the non-resonant continuum (n=1,2,3,4) are denoted by $L_{+}^{(n)}$.

c^2	0_1^+	2_1^+
$0p_{3/2}^4$	0.30–i1.32	0
$0p_{3/2}^3 0p_{1/2}^1$	0	0.81–i0.77
$0p_{3/2}^2 0p_{1/2}^2$	–0.06–i0.16	–0.01–i0.03
$L_{+}^{(1)}$	1.60+i1.07	0.45 +i0.66
$L_{+}^{(2)}$	–0.73+i0.63	–0.21+i0.16
$L_{+}^{(3)}$	–0.13–i0.20	–0.03–i0.24
$L_{+}^{(4)}$	–0.02–i0.01	$\sim$0

CONCLUSIONS

In conclusion, the complex energy Berggren ensemble is applied for the first time in shell-model calculations for many-neutron states near the particle-emission threshold. In addition to the successful inclusion of the continuum-continuum coupling, we succeeded in solving another principal problem of the GSM, i.e., the treatment of the non-

resonant part of the continuum. Another problem which has been solved in our work is the selection of resonance states. As a result of the GSM diagonalization, one obtains a multitude of states corresponding to the many-body continuum, some being resonances and some representing the non-resonant background. Our work offers a simple prescription on how to identify the resonance states.

The results of our pilot calculations are very encouraging. It is seen that the contribution from the non-resonant continuum is important, especially for bound and near-threshold states. In particular, pairing correlations due to the continuum-continuum scattering can bind the ground states of ^{6,8}He with a completely unbound basis provided by the s.p. resonances of ^{5}He. In all cases considered, calculations yield neutron resonances above the calculated neutron threshold – a property that is not guaranteed *a priori* by the formalism. Other applications of GSM, including the case of open proton *and* neutron shells, are in progress.

ACKNOWLEDGMENTS

This work was supported in part by the U.S. Department of Energy under Contract Nos. DE-FG02-96ER40963 (University of Tennessee) and DE-AC05-00OR22725 with UT-Battelle, LLC (Oak Ridge National Laboratory).

REFERENCES

1. Casten, R.F. *Nuclear Structure from a Simple Perspective* (Oxford University Press, Oxford 1990).
2. Nazarewicz, W. and Casten, R.F., *Nucl. Phys.* A **682**, 295c (2001); Casten, R.F. and Sherrill, B.M., *Prog. Part. Nucl. Phys.* **45**, S171 (2000).
3. Dobaczewski, J. and Nazarewicz, W., *Phil. Trans. R. Soc. Lond.* A **356**, 2007 (1998).
4. Fano, U., *Phys. Rev.* **124**, 1866 (1961); Mahaux, C. and Weidenmüller, H.A., *Shell-model approach to nuclear reactions* (North-Holland, Amsterdam, 1969).
5. Bennaceur, K. *et al.*, *Nucl. Phys.* A **651**, 289 (1999); ibid. A **671**, 203 (2000); Bennaceur, K. *et al.*, *Phys. Lett.* **B488**, 75 (2000).
6. Danilin, B.V. *et al.*, *Nucl. Phys.* A **632**, 383 (1998); Nielsen, E. *et al.*, *Phys. Rep.* **347**, 373 (2001); Esbensen, H. and Bertsch, G.F., *Phys. Rev.* C **59**, 3240 (1999).
7. Michel, N., Nazarewicz, W., Płoszajczak, M. and Bennaceur, K., *Phys. Rev. Lett.* (2002), in press.
8. Betan, R.I. *et al.*, *Phys. Rev. Lett.* (2002), in press.
9. Gamow, G., *Z. Phys.* **51**, 204 (1928); Siegert, A.F.J., *Phys. Rev.* **56**, 750 (1939).
10. Berggren, T., *Nucl. Phys.* A **109**, 265 (1968); *Nucl. Phys.* A **389**, 261 (1982).
11. Lind, P., *Phys. Rev.* C **47**, 1903 (1993).
12. Vertse, T., Curutchet, P. and Liotta, R.J., *Lecture Notes in Physics* **325** (Springer Verlag, Berlin 1987), p. 179; Dussel, G.G. *et al.*, *Phys. Rev.* C **46**, 558 (1992).
13. Vertse, T., Liotta, R.J. and Maglione, E., *Nucl. Phys.* A **584**, 13 (1995).
14. Lind, P. *et al.*, *Z. Phys.* A **347**, 231 (1994).
15. Liotta, R.J. *et al.*, *Phys. Lett.* B **367**, 1 (1996); Vertse, T. *et al.*, *Phys. Rev.* C **57**, 3089 (1998).
16. Michel, N., Nazarewicz, W., Płoszajczak , M., and Okołowicz, J., to be published.